STARS

University of Central Florida
STARS

Faculty Bibliography 2000s

Faculty Bibliography

1-1-2004

Broadband optical limiter based on nonlinear photoinduced anisotropy in bacteriorhodopsin film

Yuhua Huang
University of Central Florida

Georgios Siganakis
University of Central Florida

M. G. Moharam
University of Central Florida

Shin-Tson Wu
University of Central Florida

Find similar works at: https://stars.library.ucf.edu/facultybib2000

University of Central Florida Libraries http://library.ucf.edu

Recommended Citation

University of Central Florida

STARS
Showcase of Text, Archives, Research & Scholarship

Yuhua Huang, Georgios Siganakis, M. G. Moharam, and Shin-Tson Wu

View Online   Export Citation

ARTICLES YOU MAY BE INTERESTED IN

Applied Physics Letters

Mid-IR and THz frequency combs
special collection

Read Now!

Broadband optical limiter based on nonlinear photoinduced anisotropy in bacteriorhodopsin film

Yuhua Huang, Georgios Siganakis, M. G. Moharam, and Shin-Tson Wu[a)]
College of Optics and Photonics, University of Central Florida, Orlando, Florida 32816

Nonlinear photoinduced anisotropy in a bacteriorhodopsin film was theoretically and experimentally investigated and a broadband active optical limiter was demonstrated in the visible spectral range. A diode-pumped second harmonic yttrium aluminum garnet laser was used as a pumping beam and three different wavelengths at $\lambda = 442$, 532, and 655 nm from different lasers were used as probing beams. The pump and probe beams overlap at the sample. When the pumping beam is absent, the probing beam cannot transmit the crossed polarizers. With the presence of the pumping beam, a portion of the probing light is detected owing to the photoinduced anisotropy. Due to the optical nonlinearity, the transmitted probing beam intensity is clamped at a certain value, which depends on the wavelength, when the pumping beam intensity exceeds 5 mW/mm^2. Good agreement between theory and experiment is found. © *2004 American Institute of Physics.* [DOI: 10.1063/1.1828590]

An optical power limiter (OPL) is a nonlinear optical device in which its transmittance depends on the incident light intensity. In the low intensity region, the output beam intensity is linearly proportional to the input intensity. However, as the input intensity increases the output intensity gradually saturates. It is a useful device for protecting human eyes and optical sensors from being damaged by lasers. Various materials with large optical nonlinearity and high stability have been extensively investigated for optical limiting applications.[1,2] In addition to organic and inorganic crystals, biological molecules have also been explored for such applications. Among them, bacteriorhodopsin (bR), a photochromic protein in the purple membrane of halobacterium halobium, has attracted the most attention because of its unique optical properties such as large optical nonlinearity and excellent thermal- and photostabilities. Several techniques, e.g., nonlinear absorption,[3] self-diffraction,[4] and nonlinear birefringence,[5] have been used to demonstrate the optical limiting behavior in a bR film. However, these devices are narrow band. With continuous development of wavelength tunable and high power laser sources, broadband optical power limiters are needed.

Two types of OPL have been developed: passive and active. For a passive OPL, only one laser beam is involved. The transmittance of the OPL decreases as the incident beam intensity increases. However, for an active OPL the device could be controlled by a second beam (pump-probe system) or by an applied voltage. In this letter, we demonstrate a broadband active OPL using the nonlinear photoinduced anisotropy in a bR film. Unlike other approaches, the active OPL based on photoinduced optical anisotropy in bR can be used in the whole visible spectral range. The reason is that photoinduced anisotropy is comprised of photoinduced dichroism predominating around the absorption peak and photoinduced birefringence predominating in the off-resonance region. Since bR exhibits a broadband absorption in the visible range, as shown in Fig. 1, its photoinduced anisotropy covers the whole visible region. We theoretically and experimentally investigate the nonlinear performance of

photoinduced anisotropy in bR at red, green, and blue wavelengths. Good agreement between theory and experiment is obtained.

To understand the photoinduced anisotropy in bR, we need to consider its photophysical processes after the illumination of a linearly polarized light. Initially, molecules are randomly distributed in the bR film, as shown in Fig. 2(a). Upon excitation of a linearly polarized light, those bR molecules (darker color) with the dipole moment aligned close to the polarization direction of the illumination beam are pumped to the excited state and produce photoisomerization from *all trans* to 13-*cis*.[7] Then the excited molecules go through several spectroscopically distinguished intermediate states (K, L, M, N, and O) and the corresponding excited states, and relax back to the initial state spontaneously.[7,8] Due to the change of molecular structure, the refractive index and absorption coefficient of the bR molecules along the pump beam polarization axis change with the formation of each intermediate state, however, those in the perpendicular direction do not change. Therefore, macroscopic anisotropy of the bR film is induced by the illuminating light. Since the Br and M states have much longer lifetimes than other intermediate states in the photocycle, we could only consider Br and M states and their corresponding excited states,[9] as shown in Fig. 2(b). Here we regard the intermediate M state as M_G and the corresponding excited state as M_E. To analyze
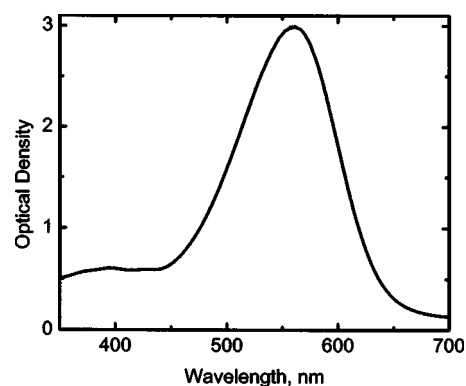

FIG. 1. The optical density of a bR film. $d = \sim 80$ μm.

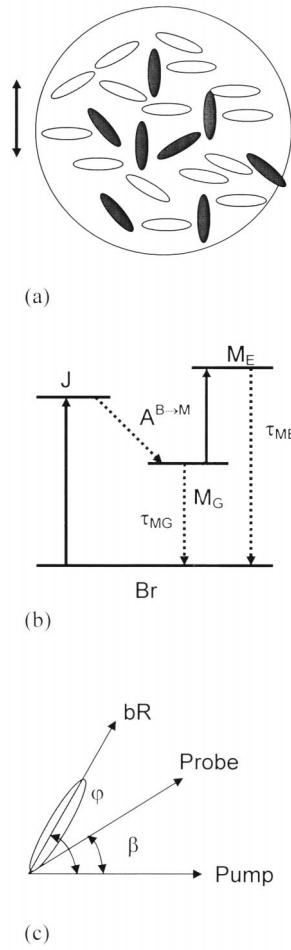[a)]Electronic mail: swu@mail.ucf.edu

(a)

(b)

(c)

FIG. 2. An illustration interpreting (a) photoselection of molecules under linearly polarized light, (b) simplified energy-level mode, and (c) angle configuration of the bR molecules and the pumping and probing beams.

the photoinduced anisotropy in bR films, linearly polarized pumping and probing beams are assumed. In Fig. 2(c), we define the polarization direction of the pumping beam as horizontal axis and that of the probing light at an angle β. For those molecules at angle φ, the population of a Br state can be described as follows:

$$
\frac{dN_{Br}(\varphi)}{dt} = -\left(\frac{\sigma_{Br-probe}A^{B \to M}I_{probe}}{h\nu_{probe}} \right.
$$
$$
+ \left. \frac{\sigma_{Br-pump}A^{B \to M}I_{pump}}{h\nu_{pump}} \right)N_{Br}(\varphi)
$$
$$
+ \frac{N_{M_G}}{\tau_{M_G}} + \frac{N_{M_G}(\varphi)}{\tau_{M_E}}. \tag{1}
$$

In Eq. (1), $N_{Br}(\varphi)$, $N_{M_G}(\varphi)$, and $N_{M_E}(\varphi)$ are the population density of the Br, ground, and excited M state along φ direction, respectively, h is the Planck constant, $\nu_i = C/\lambda_i$ is the probing and pumping beam frequency, and $A^{B \to M} = 0.64$ is the quantum efficiency for the transition from Br ground state to the excited state,[6] $\sigma_{Br-probe}$, $\sigma_{M-probe}$, $\sigma_{Br-pump}$, and σ_{M-pump} are the effective absorption cross section of bR's Br and M states at the probing and pumping wavelengths, respectively. They can be described as follows:[10]
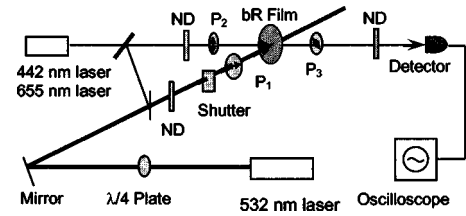

FIG. 3. Experimental apparatus for investigating photoinduced anisotropy in a bR film. P_1, P_2, and P_3 are polarizers: P_2 and P_3 are crossed, P_1 is at 45° with respect to P_1. ND: neutral density filter.

$$
\sigma_{i-j} = \sigma_{i-j}^{\parallel} \cos^2(\varphi - \beta) + \sigma_{i-j}^{\perp} \sin^2(\varphi - \beta), \tag{2}
$$

where $\sigma_{i-j}^{\parallel}$ and $\sigma_{i-j}^{\perp}$ present the parallel and perpendicular absorption cross section of each state at the probing and pumping wavelengths, respectively, i represents the Br and M_G states, and j represents the probe and pump beams, respectively.

According to the energy-level theory, the total population density N of the bR film and the population density of the Br, M_G, and M_E states should satisfy the following relationship: $N_{Br} + N_{M_G} + N_{M_E} = N$. Similarly, the relationship of N and the population density of each state at angle φ should be $N_{Br}(\varphi) + N_{M_G}(\varphi) + N_{M_E}(\varphi) = N/2\pi$. Since the M_E state has a much shorter lifetime than the Br and M_G states, fewer populations can stay in the M_E state. As a result, the M_E state population can be ignored and the population of the M_G state can be simplified as $N_{M_G} = N/2\pi - N_{Br}$.

The photoinduced birefringence and dichroism can be generally described as follows:

$$
\Delta n = \Delta n_{Br} \int_0^{2\pi} N_{Br}(\varphi)(\cos \varphi - \sin \varphi)d\varphi
$$
$$
+ \Delta n_{M_G} \int_0^{2\pi} N_{M_G}(\varphi)(\cos \varphi - \sin \varphi)d\varphi, \tag{3}
$$

$$
\Delta D = d \log(e) \left[(\sigma_{Br-probe}^{\perp} - \sigma_{Br-probe}^{\parallel}) \int_0^{2\pi} N_{Br}(\varphi) \right.
$$
$$
\times (\cos^2 \varphi - \sin^2 \varphi)d\varphi + (\sigma_{M_G-probe}^{\perp} - \sigma_{M_G-probe}^{\parallel})
$$
$$
\times \left. \int_0^{2\pi} N_{M_G}(\varphi)(\cos^2 \varphi - \sin^2 \varphi)d\varphi \right]. \tag{4}
$$

In Eq. (4), ΔD represents the effective photoinduced dichroism. Δn, Δn_{Br}, and Δn_{M_G} present the effective photoinduced birefringence, the photoinduced birefringence per molecule of the Br and M_G states, respectively. Considering the photoinduced dichroism and birefringence, the corresponding transmitted probe beam intensity I_{out} can be generally written as

$$
I_{out} = I_{in}10^{-\Delta D}\sin^2(2\beta)\sin^2(\pi\Delta nd/\lambda_{probe})
$$
$$
\times \exp^{-(\sigma_{Br-probe}^{\parallel}N_B + \sigma_{M_G-probe}^{\parallel}N_M)d}, \tag{5}
$$

where I_{in} is the incident probe beam intensity, λ_{probe} is the probing beam wavelength, and d is the film thickness.

Figure 3 shows the experimental apparatus. A linearly polarized diode-pumped Nd-Yttrium aluminum garnet (YAG) laser ($\lambda = 532$ nm) was converted to circularly polarized light by a quarter-wave plate and then split into two beams by a beam splitter. One of the green beams was used

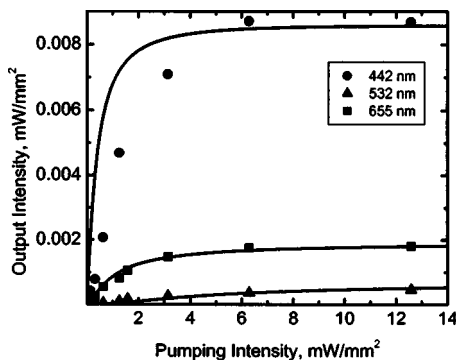Appl. Phys. Lett., Vol. 85, No. 22, 29 November 2004

Huang *et al.* 5447

FIG. 4. Pumping beam intensity dependent on transmitted probing beam intensity. Dots are experimental data and solid lines are simulation results using Eq. 10. In our simulation, we use $\sigma_B^\parallel$=0.1, 1.6, and 0.2×10^{-16} cm^2 at λ=655, 532, and 442 nm, respectively; $\sigma_M^\parallel$=0, 3.8×10^{-18}, and 0.4×10^{-16} cm^2 at λ=655, 532, and 442 nm, respectively; $\sigma_i^\parallel/\sigma_i^\perp$=10, τ_{MG}=0.2 s, and τ_{ME}=1 ns.

as a pumping beam. A linear polarizer P_1 was used to select the desired polarization state. The other green beam, a blue He-Cd laser (λ=442 nm), and a red diode laser (λ=655 nm) were used as probing beams. The pumping beam overlaps with the probing beam at the bR film which was sandwiched between a pair of crossed Glan-Thompson polarizers P_2 and P_3. The polarization direction of the pumping beam selected by P_1 is inclined at 45° with respect to P_2. The bR samples were purchased from Munich Innovative Biomaterials GmbH (order number WT1N3). Its thickness is ~80 μm and optical density is 3 at λ=570 nm.

Without pumping beam, the probing beam could not transmit the analyzer P_3 because the bR film is isotropic. With the presence of the pumping beam, the analyzer P_3 transmits a portion of the probing light due to the photoinduced anisotropy in the bR film. The transmitted probing beam intensity highly relies on the pumping beam intensities, as shown in Fig. 4. Figure 4 shows the pumping beam intensity dependent on transmitted probing beam intensity when the probing beam (λ=442, 532, and 655 nm) intensity was set at 0.45, 0.28, and 0.39 mW/mm^2, respectively. In the low pumping intensity regime, the transmitted probing beam intensity increases almost linearly with the increasing pumping beam intensity. However, as the pumping intensity reaches ~5 mW/mm^2, the transmitted probe beam intensity starts to saturate. In the higher intensity regime, the probing beam intensity is clamped to a saturation level. The response time is about 200 ms.

Using the theoretical model described above, we can simulate the experimental results. Based on the absorption spectra published in Ref. 11, we estimated that $\sigma_{Br}^\parallel$=0.1, 1.6, and 0.2×10^{-16} cm^2, and $\sigma_M^\parallel$=0, 3.8×10^{-18}, and 0.4×10^{-16} cm^2 at λ=655, 532, and 442 nm, respectively. In our simulations, we assume the dichroic ratio of the Br and M states is $\sigma_i^\parallel/\sigma_i^\perp$=10. Varying the dichroic ratio from 10 to 100 does not affect the calculated results noticeably. In addition, from our experiment we found τ_{MG}=0.2 s. The lifetime of the excited M state is commonly known to be τ_{ME} ~1 ns.[6] The simulation results are shown as the solid lines in Fig. 4. The agreement between theory and experiment is good.

From Eqs. (3)–(5), the transmitted probe beam intensity is determined by the photoinduced anisotropy which is proportional to the number of the excited bR molecules. Since the number of the excited state molecules is linearly proportional to the pumping beam intensity in the low intensity regime and saturates in the high intensity regime, the transmitted probe beam intensity should have the same trend. Since bR has a larger absorption cross section at λ=532 nm than that at 442 and 655 nm, the perpendicular transmittance of the probe beam at λ=532 nm is lower than that at 442 and 655 nm. Equation (5) also indicates that the transmitted probe beam intensity increases with the incident probe beam intensity. Therefore, different applications can be realized at different incident probe beam intensities. For example, by choosing a proper incident probe beam intensity, the device can be used for laser eye protection. This is another advantage in comparison with the previously proposed optical limiters using bR material besides the aforementioned broad bandwidth. Using Eq. (5), we calculated the photoinduced birefringence to be Δn ~1.79, ~1.3, and ~4.87 $\times10^{-4}$ at λ=655, 532, and 442 nm, respectively. These data are the same order of magnitude as those reported in Refs. 5 and 12.

For optical limiter applications, the device should be able to respond immediately to the environmental condition. The response time of our sample is slow (~200 ms) due to the long M-state lifetime but it can be improved by changing the temperature, humidity, or pH value. It is known that the bR response time in water solution is ~10 ms. Our studies on the temperature effect indicate that the response time decreases with the increasing temperature. At ~50 °C, the bR response time in water solution is reduced to ~3 ms, which is much faster than other organic photochromic materials such as fulgide.[13]

In conclusion, we have investigated the nonlinear photoinduced anisotropy in bR film and demonstrated an active optical limiter based on it. The device can be used in the whole visible region. By choosing a suitable incident probing beam intensity, the device can be used for laser eye protection. The device response time is slow (~200 ms), which is due to the long lifetime of the M state. The M-state lifetime can be significantly reduced to ~3 ms by changing the temperature, pH value, and humidity during fabrication process.

[1] H. B. Lin, R. J. Tonucci, and A. J. Campillo, Opt. Lett. **23**, 94 (1998).
[2] G. Poirier, C. B. de Araujo, Y. Messaddeq, S. J. L. Ribeiro, and M. Poulain, J. Appl. Phys. **91**, 10221 (2002).
[3] Q. W. Song, C. Zhang, R. Gross, and R. Birge, Opt. Lett. **18**, 775 (1993).
[4] D. N. Rao, C. S. Yelleswarapu, S. R. Kothapalli, D. V. G. L. N. Rao, and B. R. Kimball, Opt. Express **22**, 2848 (2003).
[5] G. E. Dovgalenko, M. Klotz, G. J. Salamo, and G. L. Wood, Appl. Phys. Lett. **68**, 287 (1996).
[6] Y. H. Huang, S. T. Wu, and Y. Y. Zhao, Appl. Phys. Lett. **84**, 2028 (2004).
[7] R. R. Birge, Annu. Rev. Biophys. Bioeng. **10**, 315 (1981).
[8] Y. H. Huang, S. T. Wu, and Y. Y. Zhao, Opt. Express **12**, 895 (2004).
[9] T. H. Zhang, C. P. Zhang, G. H. Fu, Y. D. Li, L. Q. Gu, G. Y. Zhang, Q. W. Song, B. Parsons, and R. R. Birge, Opt. Eng. (Bellingham) **39**, 527 (2000).
[10] E. Y. Korchemskaya, D. A. Stepanchikov, A. B. Druzhko, and T. V. Dyukova, J. Biol. Phys. **24**, 201 (1999).
[11] J. A. Stuart, D. L. Mercy, K. L. Wise, and R. R. Birge, Synth. Met. **127**, 3 (2002).
[12] Q. W. Song, Y. H. Zhang, R. R. Birge, and J. D. Downie, Proc. SPIE **3470**, 226 (1998).
[13] M. Seibold and H. Port, Chem. Phys. Lett. **252**, 135 (1996).